Physica A 415 (2014) 538–543

Contents lists available at ScienceDirect

Physica A

journal homepage: www.elsevier.com/locate/physa

Fractals and self-organized criticality in anti-inflammatory drugs

J.C. Phillips *

Department of Physics and Astronomy, Rutgers University, Piscataway, NJ, 08854, United States

HIGHLIGHTS

- There are two kinds of aspirin; both act by inhibiting a certain catalytic activity.
- Large medical differences are unexplained at the molecular level.
- Fractals quantify bicyclic imbalances of large-scale hydropathic forces.
- Success made possible by a new record of 25 decades for fractal content.
- Natural surface mutations can modify bicyclic imbalances.

ARTICLE INFO

Article history:
Received 19 March 2014
Received in revised form 11 July 2014
Available online 20 August 2014

Keywords:
Globular
Roughness
Length
Profile
Function
Engineer

ABSTRACT

Nonsteroidal anti-inflammatory drugs (NSAIDs) act through inhibiting prostaglandin synthesis, a catalytic activity possessed by two distinct cyclooxygenase (COX-1 and COX-2) isozymes encoded by separate genes. The discovery of COX-2 launched a new era in NSAID pharmacology, resulting in the synthesis, marketing, and widespread use of COX-2 selective inhibitors. Extensive structural studies of the biology of prostaglandin synthesis and inhibition have explained some of the differences between COX-1 and COX-2 functionality, but others are still unexplained. Notably these include molecular differences that cause COX-1 inhibitors to produce a slight decrease, and COX-2 inhibitors to induce a significant increase, in heart attacks and strokes. These differences were unexpected because of the 60% overall COX-1 and COX-2 sequence similarity and the 1–2 conservation of catalytic sites. Hydropathic analysis shows important bicyclic differences between COX-1 and COX-2 on a large scale outside the catalytic pocket. These differences involve much stronger amphiphilic interactions in COX-2 than in COX-1, and may explain the selective antiplatelet effectiveness of COX-2. Success of the non-Euclidean structural analysis is the result of using the new Brazilian hydropathicity scale based on self-organized criticality (SOC) of universal protein modules.

1. Introduction

Aspirin (acetylsalicylic acid or ASA) is probably the oldest drug (its uses stretch back to antiquity, though pure ASA has been manufactured and marketed only since 1899), see Wiki on history of aspirin. In 1971 Vane discovered the mechanism by which aspirin exerts its anti-inflammatory, analgesic and antipyretic actions. Aspirin and other non-steroid anti-inflammatory drugs (NSAIDs) inhibit the activity of cyclooxygenase (COX) which leads to the formation of prostaglandins

* Tel.: +1 908 273 8218.
E-mail address: jcphillips8@comcast.net.

http://dx.doi.org/10.1016/j.physa.2014.08.032
0378-4371/

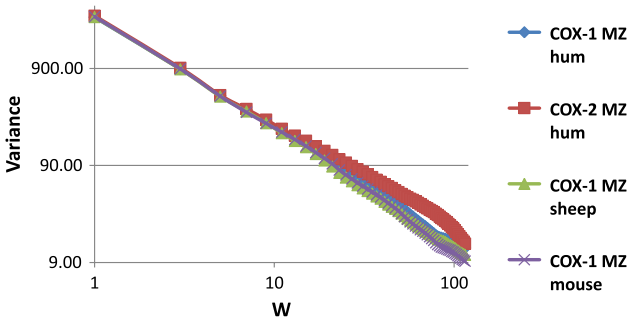

Fig. 1. Variances $\mathcal{R}(W)$ for COX-1 for several species and COX-2 human. For large W the differences are larger, and the evolutionary trends (mouse–sheep–human) of COX-1 become monotonic. The small differences shown here are enhanced in Fig. 2 by comparing variance ratios. Ratios can also be applied successfully to monitoring evolutionary advances in functionality, and identifying optimal values of W [6,7].

(PGs) that cause inflammation, swelling, pain and fever. However, by inhibiting this key enzyme in PG synthesis, the aspirin-like drugs also prevent the production of physiologically important PGs which protect the stomach mucosa from damage by hydrochloric acid, maintain kidney function and aggregate platelets when required. This conclusion provided a unifying explanation for the therapeutic actions and shared side effects of the aspirin-like drugs. Daniel Simmons discovered the COX-2 enzyme in 1988, and Harvey Herschman discovered a COX-2 gene in 1991. The constitutive isoform, COX-1, supports the beneficial homeostatic functions, whereas the inducible isoform, COX-2, becomes upregulated by inflammatory mediators [1].

COX-2 inhibitors became attractive when it was realized that they could have the same anti-inflammatory, anti-pyretic, and analgesic activities as nonselective inhibitors NSAIDs, with little or none of the gastrointestinal side-effects [2]. However, the most important difference between COX-1 and COX-2 inhibitors is the appearance of significant cardiovascular toxicity associated with chronic use (2%–4% of patients after 3 years) of COX-2. This difference remains unexplained, although there are few enzymes of lipid biochemistry for which there is such a wealth of structural and functional information [3]. However, this structural information is limited to COX complexed with inhibitors, which are known to strain the wild structures [4].

Given that only 50% sequence identity is enough to make the backbone coordinates of chicken and human lysozyme *c* superposable to 1.5 A [5], the larger 60%–65% sequence identity of COX-1 and COX-2 should be enough to prevent elucidation of their functional differences from structural data alone [2]. However, Ref. [5] found that the evolutionary trends from chicken to human of compensating enzymatic and lytic properties of lysozyme *c* were explicable from analysis of their amino acid (aa) sequences alone, by evaluating their hydroanalytic profiles and modular correlations. These new methods extract a wealth of information from (aa) sequences alone, by using scaling to obtain amino acid hydropathicities. The latter describe water–protein interactions in a quasi-one-dimensional non-Euclidean space quite different from conventional Euclidean three-dimensional structural models. Because the description has both evolutionary and thermodynamic aspects, it yielded many accurate results both for amyloid precursor A4 (770 aa) [6] and amyloid beta (40 aa) [7] unobtainable from conventional Euclidean structural models alone.

Here we use similar hydroanalytic methods to analyze functional differences between COX-1 and COX-2 in terms of the human amino acid sequences Uniprot P23219 COX-1, 599 aa, and COX-2, 604 aa, P35354. In earlier work we found that the best single descriptor of small differences between similar proteins is given by their roughnesses $\mathcal{R}(W)$ or variances of $\psi(\text{aa}, W)$, where $\psi(\text{aa}, W)$ is $\psi(\text{aa}, 1)$ averaged over a sliding window of length W centered on consecutive aa. Here $\psi(\text{aa}, 1)$ is a hydropathicity value from one of two scales, the KD scale [8], which corresponds to complete (water–air) unfolding, and has first-order thermodynamic character, and the Brazilian MZ scale based on modular surface areas obtained from Voronoi partitioning [9], which has second-order character and reflects both evolutionary and thermodynamic aspects of protein optimization. The MZ scale has yielded consistently much more accurate sequence-functional results [5, 6.7], which is not surprising, as it is ideally suited to describing conformational changes and how these change protein packing.

2. Optimizing the length scale *W*

Because of the large sequence identity of COX-1 and COX-2, it may appear difficult to analyze their differences quantitatively. However, their similarity can be turned to advantage by comparing their overall roughnesses or sequence variances $\mathcal{R}(W)$ in Fig. 1. We see that the $\mathcal{R}(W)$ differences are small for small W, but increase with increasing W, finally peaking at $W = 79$. The meaning of this large value of W will be made clear below, but for the moment we can interpret it as an average spacing between the centers of modules that are involved in critical large-scale conformational changes that distinguish COX-1 from COX-2.

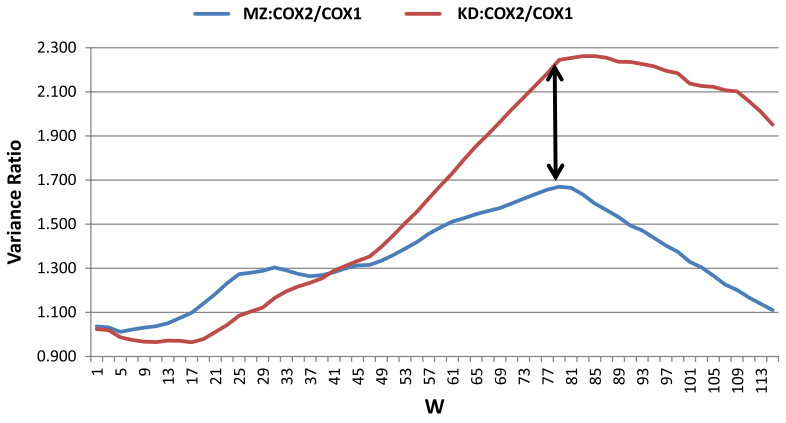

Fig. 2. The ratio of COX2/COX1 $\Re(W)$ roughnesses (variances) is shown for two scales, KD (first-order) and MZ (second-order). For both scales the ratio is maximized by choosing $W = 79$ (double arrow). There are multiple reasons for preferring the MZ scale. Its peak is more symmetrical, and the KD scale appears to be noisy above $W = 79$. Also the secondary peak near $W = 25$, which is presumably associated with membrane interactions, is clear for the MZ scale, but broadened and almost invisible for the KD scale. Overall this process can be compared to adjusting the focus on a microscope to optimize the COX-1 and COX-2 differences (here we are looking at, in effect, the dynamical differences between the two water–protein interfaces).

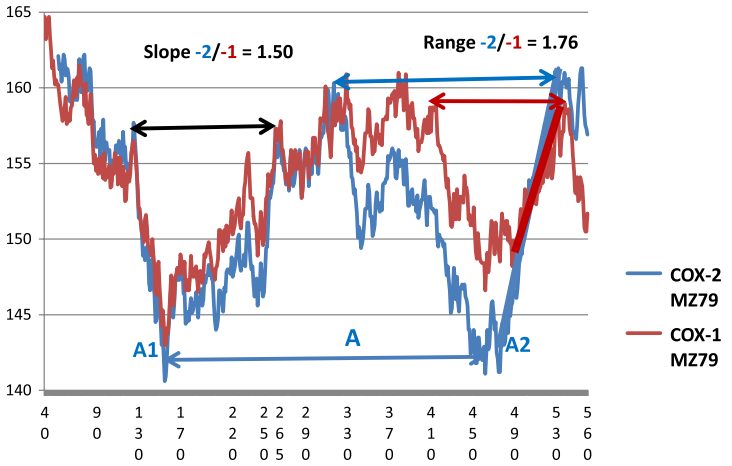

Fig. 3. The MZ hydroprofiles of COX-1 and COX-2 with $W = 79$ are similar in the sense that the 600 aa proteins are divided into two parts of nearly equal length separated by central hydrophobic peaks. Each N- and C-part contains a deep hydrophilic hinge, labeled A1 and A2 respectively. Closer inspection reveals multiple COX-1 and COX-2 differences of four types: the large difference in range of the amphiphilic modules that contain the catalytic channel, indicated by the lines to guide the eye near site 500; the leveling or balancing of hydrophobic peaks near 530 with hydrophobic peaks near 410 (COX-1) and 300 (COX-2), indicated by the double colored arrows; the third point, R108Q mutational effects, is marked by the black double arrow centered near 200. The fourth point and most striking point concerns the balancing A of the two deepest N- and C-hydrophilic hinges A1 (near 150) and A2 (near 460), which occurs only for COX-2. These profiles are based on the COX-1 and COX-2 Uniprot sequences, but the COX-2 sequence has been aligned with the COX-1 sequence by displacing it by 13 aa, as indicated by BLAST. (For interpretation of the references to color in this figure legend, the reader is referred to the web version of this article.)

3. Large-scale profiles

According to Fig. 2, the COX-1 and COX-2 $\Re(W)$ variance differences, which are only 3% for $W = 1$, reach 50% with the more accurate MZ scale at $W = 79$. In Fig. 3 COX-1 and COX-2 profiles are shown with $W = 79$, which identify the variance differences associated with the amphiphilic modules that contain the catalytic entrance region near 500–520. Three other differences are marked, associated with leveling of hydrophobic and hydrophilic extrema, which stabilizes central and surface aa configurations which have been partitioned by the Voronoi construction [9,10].

Probably the most important feature of Fig. 3 is the large-scale balancing of the two deepest hydrophilic minima near 150 and 460, which occurs only for COX-2. Fig. 3 also shows the slope and range ratios of COX-1 and COX-2 amphiphilic modules that contain the catalytic entrance region near 500–520. From the figure one could conjecture that the larger amphiphilic slope and range of COX-2 compared to COX-1 could be associated with the large-scale balancing A of the two deepest hydrophilic minima near 150 and 460, which occurs only for COX-2.

Fig. 2 suggested that in addition to the large-scale variance ratios due to matching of far-separated phobic and philic extrema with $W = 79$, one could also have differences due to interactions with membranes around $W = 25$ that are stronger

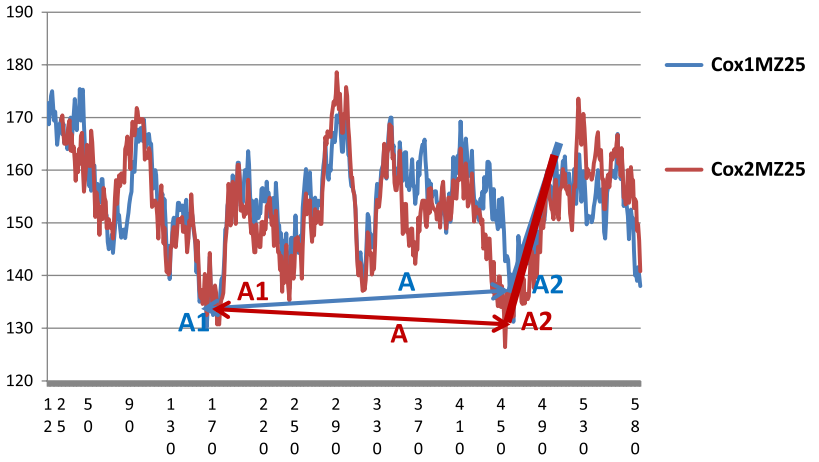

Fig. 4. The MZ profiles of COX-1 and COX-2 with $W = 25$ are also similar in the sense that the 600 aa proteins are divided into two parts of nearly equal length separated by central hydrophobic peaks near 300. Closer inspection reveals fewer differences than those with $W = 79$ done in Fig. 3. Now we note the balancing A of the two deepest hydrophilic hinges A1 (near 150) and A2 (near 460), which occurs for both COX-1 and COX-2. Here the amphiphilic modules that contain the catalytic region 460–500, indicated by the lines to guide the eye, are nearly equal in slope and length. The leveling or balancing of hydrophobic peaks near 500 with other hydrophobic peaks near 400 is unclear for $W = 25$. That the membrane length scale $W = 25$ reveals fewer COX-1 and COX-2 differences than the N- and C-hinge length scale $W = 79$ was already clear from Figs. 1 and 2.

for COX-2 than for COX-1. In Fig. 4 we can see the MZ25 profiles of COX-1 and COX-2, and compare them with the $W = 79$ profiles in Fig. 3. With $W = 25$ we still see the large-scale balancing A of the two deepest hydrophilic minima near 150 and 460, and now it occurs for both COX-1 and COX-2. At the same time the slopes and ranges of COX-1 and COX-2 amphiphilic modules for $W = 25$ are nearly equal. This is consistent with the above conjecture connecting the differing strengths of the smaller modules to the balancing of the N- and C-terminal hydrophilic hinges for the long-range value $W = 79$, which occurs only for COX-2.

4. Functions of COX-1 and COX-2

COX catalyzes prostaglandin biosynthesis by a complex series of reactions of arachidonic acid involving oxygenation, cyclization, and the generation of five chiral centers from an achiral substrate [11]. The key step is the formation of bicyclic peroxides (endoperoxides) as the initial products of polyunsaturated fatty acid oxygenation (Fig. 1 of Ref. [11]). The $W = 79$ and $W = 25$ COX profiles in Figs. 2 and 3 also have a bicyclic structure based on balanced hydrophilic hinges A1 and A2 that is ∼100 times larger than that of arachidonic acid. This structure is present for both COX-1 and COX-2 for $W = 25$ (membrane scale), but exists only for COX-2 for $W = 79$ (larger scale of platelet adhesion, see below).

These bicyclic features suggest a mechanical model for the above complex series of bicyclic reactions. At each stage the N- and C-terminal hydrophilic hinges undergo appropriate conformational changes adapted to the generation of the chiral center of that stage. These conformations are stable for the long times needed for chiral synthesis because the bicyclic COX hydrophilic hinges A1 and A2 are balanced and have stable Voronoi interfaces at the protein surface [10].

The larger scale $W = 79$ reveals bicyclic N- and C-balance for COX-2 only. When it was realized that COX-2 inhibitors produce significant cardiovascular toxicity, this was soon connected to COX-2 restriction of platelet formation, adhesion to vessel walls, and vessel occlusion [12]. It is natural to suppose that large-scale platelet kinetics can be controlled well by COX-2 and not by COX-1 ($W = 79$, see Fig. 3).

5. Comparison with Euclidean models

Strictly speaking, the detailed large-scale differences between COX-1 and COX-2 are not perceptible in Euclidean models that rely on short-range contact interactions ($W \sim 1$) between inhibitors bound to COX-1 or COX-2. However, there are some features of our non-Euclidean hydropathic model that correspond to observations made in earlier work. The correspondences are much closer with the MZ scale than with the KD scale, which adds plausibility to the similarities identified in two apparently different three-dimensional Euclidean and one-dimensional non-Euclidean interaction spaces. Following Fig. 2 of Ref. [11], the mutation Y384F can affect binding to COX-1, because there is a strong hydrophobic peak between 369 and 387 in the $W = 79$ profile of COX-1, but this peak is much reduced in COX-2.

Ref. [11] analyzed strained Euclidean models for COX-1 (sheep) and COX-2 (mouse), based on docking arachidonate near R119 and Y384, and found that their active site structures are quite similar on the short length scale of the active site. They were puzzled by "this similarity, [because] clear differences in substrate specificities exist between the two enzymes. COX-2 appears much more accommodating than COX-1 in that it oxidizes 18 carbon polyunsaturated fatty acids with much higher

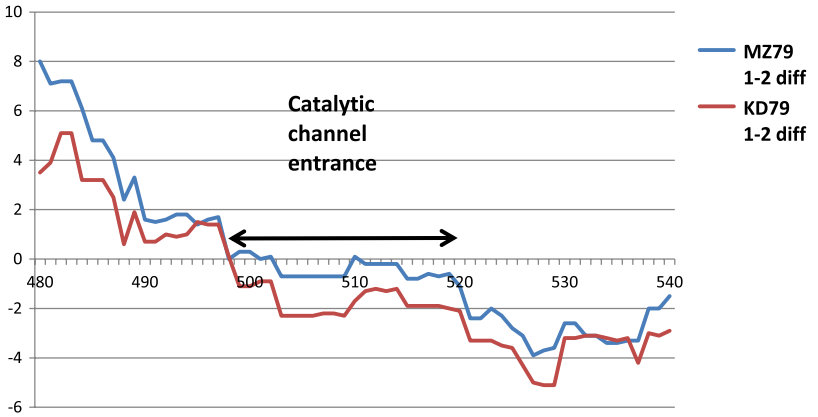

Fig. 5. The difference between COX-1 and COX-2 profiles with $W = 79$, using the MZ and KD scales, in the catalytic channel. In the hydrophilic entrance 500–520 to the hydrophobic pocket 515–535, COX-1 and COX-2 large-scale profiles are nearly identical on the MZ scale, but less so with the less accurate KD scale. The nearly exact MZ conservation of COX-1 and COX-2 profiles with $W = 79$ in this region implies what level set analysis has already told us in Fig. 3: the functional differences between these two similar proteins arise not in the catalytic channel, but across the entire bicyclic structure, especially the A1 and A2 balance for COX-2.

efficiency than COX-1. Also, COX-2 oxidizes the hydroxyethylamide derivative of arachidonic acid (anandamide) whereas COX-1 does not". It appears that the differences between the COX-1 and COX-2 hydroprofiles with the much longer length scale $W = 79$ (Fig. 3) are consistent with the much higher activity of COX-2. Ref. [11] also was puzzled by the increased activity of R119Q COX-1 mutants. Looking at Fig. 3, we see that this hydrophobic mutation on a surface site improves the balancing of the 125 and 266 peaks, and probably folds the 125 peak more deeply into the COX-1 interior, thus stabilizing conformations involving adjustments of the A1 hinge.

Refs. [2,11] and later workers [13–15] have also emphasized the structural significance of the 515–535 pocket which contains several aa that contact inhibitors in crystal structures involving COX-2 [13]. Fig. 5 displays the differences between the $M = 79$ profiles of COX-1 and COX-2 in this region. We see that in the hydrophilic channel entrance 500–520 to the hydrophobic pocket 515–535, COX-1 and COX-2 large-scale profiles are nearly identical on the MZ scale, but less so with the less accurate KD scale. The nearly exact MZ conservation of COX-1 and COX-2 profiles with $W = 79$ in this entrance implies what level set analysis has already told us in Fig. 3: the most important functional differences between these two similar proteins arise not in the catalytic channel, but across the entire bicyclic structure, especially the A1 and A2 balance for COX-2.

Ref. [14] studied four single aa mutational variants of COX-1 and found that "R108Q exerts the largest functional effects, with evidence for impaired interactions with a COX substrate and inhibitors. As Arg108 is located on the protein surface and not in the active site, the effects of R108Q suggest a novel, unsuspected mechanism for the modulation of the PGHS-1 active site structure". The black arrow in Fig. 3 marks the balancing [10] of the 125 and 265 hydrophobic peaks associated with the A1 hinge. This balance is improved by about 30% by the R108Q mutation, consistent with their observed increase of COX-1 and peroxidase (POX) catalytic parameters by a factor of 1.5. This is another example of the utility of the level set concept in the Voronoi partitioning context [9,10].

Overall the number of mutations that could be used to hybridize COX-1 with COX-2, and hopefully combine their desirable properties while minimizing the undesirable side effects, appears to be very large. One could focus on known COX-2 natural mutations that upset the A1–A2 bicyclic surface hinge balance in Fig. 3 over a range of 40 aa with $W = 79$; these should either make the 155 A1 minimum more hydrophilic, or the 453–466 A2 minimum more hydrophobic. According to Uniprot, there are only two such mutations, P428A, and E488G. The A1–A2 COX-2 difference is only 10% of the A1–A2 COX-1 difference in Fig. 3. These two mutations triple the A1–A2 COX-2 difference to 30% of the A1–A2 COX-1 difference. Most of this improvement is due to E428G, and it is large enough to warrant experimental study. The 428 site lies well away from the active sites, and like 108, it is located on the protein surface, which could be why it has not yet been studied.

6. Conclusions

Early work on COX-1 and COX-2 inhibitors found only small differences between their catalytic binding pockets, which often left important functional differences unexplained. The risk of cardiovascular events associated with selective COX-2 inhibitors was recognized early [16,17]. Marketing of several COX-2 inhibitors led to the realization of their significant cardiovascular toxicity, and market withdrawal of most COX-2 inhibitors.

The molecular mechanism for the cardiovascular toxicity of COX-2 inhibitors is unclear, with some workers ascribing it primarily to COX-2 driving vascular prostacyclin release [18], while others claim that vascular prostacyclin production in healthy blood vessels is generally driven by COX-1 [19,20]. The bicyclic structure of COX-2 identified in Fig. 3 here also

implies COX-2 fragility in vivo, so the differences between the two interpretations may not be easily resolved, especially since there are many alternatives to vascular prostacyclin elsewhere [19,21].

At the molecular level it is clear that the most important differences between COX-1 and COX-2 are not associated with differences in inhibitor binding, but with the long-range kinetic "balancing" differences of COX-1 and COX-2 described here. This conclusion is consistent with the generally agreed view that, regardless of mechanism, those drugs that inhibit COX-2 have potential deleterious effects upon cardiovascular health [19]. The present model suggests further study of the natural COX-2 mutations P428A and E488G, which could suppress cardiovascular events associated with selective COX-2 inhibitors.

References

[1] J.R. Vane, R.M. Botting, The mechanism of action of aspirin, Thromb. Res. 110 (2003) 255–258.
[2] W.L. Smith, D.L. DeWitt, R.M. Garavito, Cyclooxygenases: structural, cellular, and molecular biology, Annu. Rev. Biochem. 69 (2000) 145–182.
[3] C.A. Rouzer, L.J. Marnett, Cyclooxygenases: structural and functional insights, J. Lipid Res. 50 (2009) S29–S34.
[4] C. Luong, A. Miller, J. Barnett, et al., Flexibility of the NSAID binding site in the structure of human cyclooxygenase-2, Nature Struct. Biol. 3 (1996) 927–933.
[5] J.C. Phillips, Scaling and self-organized criticality in proteins: lysozyme *c*, Phys. Rev. E 80 (2009) 051916.
[6] M.W. Deem, J.C. Phillips, A cubic equation of state for amyloid plaque formation, 2013. arXiv:1308.5718.
[7] M.W. Deem, J.C. Phillips, Thermodynamic description of beta amyloid formation, 2013. arXiv:1310.2528.
[8] J. Kyte, R.F. Doolittle, A simple method for displaying the hydropathic character of a protein, J. Mol. Biol. 157 (1982) 105–132.
[9] M.A. Moret, G.F. Zebende, Amino acid hydrophobicity and accessible surface area, Phys. Rev. E 75 (2007) 011920.
[10] R.I. Saye, J.A. Sethian, Analysis and applications of the voronoi implicit interface method, J. Comput. Phys. 231 (2012) 6051–6085.
[11] L.J. Marnett, S.W. Rowlinson, D.C. Goodwin, et al., Arachidonic acid oxygenation by COX-1 and COX-2—mechanisms of catalysis and inhibition, J. Biol. Chem. 274 (1999) 22903–22906.
[12] M.A. Buerkle, S. Lehrer, H.Y. Sohn, et al., Selective inhibition of cyclooxygenase-2 enhances platelet adhesion in hamster arterioles in vivo, Circulation 110 (2004) 2053–2059.
[13] M.A. Windsor, P.L. Valk, X. Xu, et al., Exploring the molecular determinants of substrate-selective inhibition of cyclooxygenase-2 by lumiracoxib, Bioorg. Med. Chem. Lett. 23 (2013) 5860–5864.
[14] W. Liu, E.M. Poole, C.M. Ulrich, et al., Decreased cyclooxygenase inhibition by aspirin in polymorphic variants of human prostaglandin H synthase-1, Pharmocogen. Genom. 22 (2012) 525–537.
[15] M. Nagini, G.V. Reddy, G.R. Hemalatha, et al., Functional correlation of cyclooxygenases-1, 2 and 3 from amino acid sequences and three dimensional model structures, Indian J. Chem. A 45 (2006) 182–187.
[16] D. Mukherjee, S.E. Nissen, E.J. Topol, Risk of cardiovascular events associated with selective COX-2 inhibitors, JAMA 286 (2001) 954–959.
[17] APC Study Investigators, Cardiovascular risk associated with celecoxib in a clinical trial for colorectal adenoma prevention, N. Engl. J. Med. 352 (2005) 1071–1080.
[18] E. Ricciotti, Y. Yu, G.A. FitzGerald, COX-2, the dominant source of prostacyclin, Proc. Natl. Acad. Sci. USA 110 (2012) E183.
[19] N.S. Kirby, A.K. Zaiss, P. Urquhart, et al., LC-MS/MS confirms that COX-1 drives vascular prostacyclin whilst gene expression pattern reveals non-vascular sites of COX-2 expression, PLoS One 8 (2013) e69524.
[20] B. Liu, Y. Zhang, N. Zhu, et al., A vasoconstrictor role for cyclooxygenase-1-mediated prostacyclin synthesis in mouse renal arteries, Am. J. Physiol.-Renal Physiol. 305 (2013) CF1315-F1322.
[21] M.A. Crilly, A.A. Mangoni, K.M. Knights, Aldosterone glucuronidation inhibition as a potential mechanism for arterial dysfunction associated with chronic celecoxib and diclofenac use in patients with rheumatoid arthritis, Clin. Exp. Rheumatol. 31 (2013) 691–698.